

# Checking the error correction strength of arbitrary surface code logical gates

Thomas J. Milburn, Austin G. Fowler

*The Melbourne Quantum Computer Science Group,  
Centre for Quantum Computation and Communication Technology,  
School of Physics, the University of Melbourne, Victoria 3010, Australia*

(Dated: October 26, 2021)

Topologically quantum error corrected logical gates are complex. Chains of errors can form in space and time and diagonally in spacetime. It is highly nontrivial to determine whether a given logical gate is free of low weight combinations of errors leading to failure. We report a new tool Nestcheck capable of analyzing an arbitrary topological computation and determining the minimum number of errors required to cause failure.

## I. INTRODUCTION

Constructing a quantum device for simulating quantum systems was first suggested by Feynman in 1982 [1]. The specific device he proposed, however, was not software programmable. The first proposal for a programmable quantum computer was given by Deutsch in 1985 [2]. The paradigm of quantum computation was thus born, but it had yet to acquire motivation. This came in 1994 with the advent of Shor's factoring algorithm [3].

A concern raised early within the quantum computation community was that of its infeasibility due to decoherence [4]. Although this concern has yet to be eliminated, it has been considerably lessened. With the invention of quantum error correction in 1995 [5, 6] and the proof of the threshold theorem in 1996 [7, 8] there is now a focus on constructing quantum error correction codes.

Topological approaches to quantum error correction are particularly promising [9–13]. One such class is surface codes. The specific surface code we consider in this paper is explained well in [14]. The elementary systems of the surface code are physical qubits (two level quantum systems) [15], and the information elements are logical qubits (encoded over the physical qubits). This code allows efficient implementation of quantum algorithms and its physical requirements are modest: a 2D lattice of qubits, nearest neighbor interactions, parallelizability, and gate error rates around 1% [16, 17].

During computation, various gates are continually performed on the physical qubits with each gate having an error rate. These errors can form chains in space and time and diagonally in spacetime. Determining the error correction strength of a proposal for a surface code logical gate, which may consist of many of physical operations, can thus be somewhat complex. It can only reliably be accomplished via directly simulating the logical gate.

We report a new tool for this task: Nestcheck. Using Nestcheck we are able to analyse an arbitrary surface code logical gate and determine the minimum number of errors required to cause failure.

## II. THE SURFACE CODE

Group theoretic concepts provide a convenient formalism for describing both the logical qubits and gates of the surface code [18, 19]. Homology also lends itself to our subject [12, 20], but encasing our discussion in the terms of homology might render it inaccessible. The following is an extremely brief account of the surface code.

Consider a set of  $n$  qubits,  $\mathcal{Q}$ . Decoherence of  $|\mathcal{Q}\rangle$  is due to  $\mathcal{Q}$  interacting with an unmonitored bath,  $\mathcal{B}$ . This may be written  $U(|\mathcal{Q}\rangle|B\rangle)$ , where  $U$  is a unitary operator. The effective reduced density operator is then

$$\rho_{\mathcal{Q}} = \text{tr}_{\mathcal{B}}(U|\mathcal{Q}\rangle|B\rangle\langle\mathcal{Q}|\langle B|U^{\dagger}) = \sum_{E \in \mathcal{E}} E|\mathcal{Q}\rangle\langle\mathcal{Q}|E^{\dagger}, \quad (1)$$

where  $\mathcal{E}$  are Krauss operators. We call  $\mathcal{E}$  the errors and often relax the Krauss normalization condition [21]. By Eq. 1 and the linearity of quantum mechanics, in order to correct decoherence we need only correct a basis for  $\mathcal{E}$  [22]. A convenient choice is the complete pauli basis,  $\mathcal{G} = \{1, -1, i, -i\} \times \{I, X, Y, Z\}^{\otimes n}$ . This is a group under multiplication.

The stabilizer of  $|\mathcal{Q}\rangle$  is the set of operators  $\mathcal{S} \subset \mathcal{G}$  such that  $\mathcal{S}|\mathcal{Q}\rangle = |\mathcal{Q}\rangle$ . Every element of  $\mathcal{G}$  either commutes or anticommutes with each other element. Consider some  $S \in \hat{\mathcal{S}}$  (a generating set for  $\mathcal{S}$ ) and applying an operator  $G \in \mathcal{G}$ : If  $[G, S] = 0$  then  $SG|\mathcal{Q}\rangle = G|\mathcal{Q}\rangle$  and measuring  $S$  yields 1, whereas if  $\{G, S\} = 0$  then  $SG|\mathcal{Q}\rangle = -G|\mathcal{Q}\rangle$  and measuring  $S$  yields  $-1$ .

The surface code is a stabilizer code: we enforce a certain set of operators to be  $\hat{\mathcal{S}}$ , a set of stabilizer generators. We construct it such that every sufficiently low-weight and distinct error anticommutes with a unique subset of the phase factor 1 version of  $\hat{\mathcal{S}}$ . At regular intervals we measure the phase factor 1 version of  $\hat{\mathcal{S}}$ , each called a round of error correction. This yields an ordered set of 1s and  $-1$ s, which we call a syndrome. We call an element of a syndrome a syndrome result. If one syndrome differs from another then there has been either measurement or physical qubit error on some number of physical qubits. Assuming only those low-weight errors mentioned above, we can determine from syndrome changes the errors that caused them.

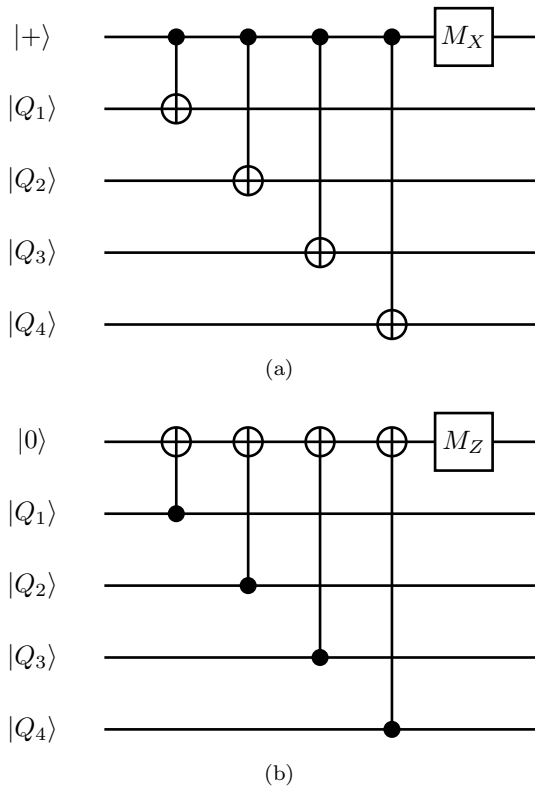


FIG. 1: Quantum circuits for measuring (a)  $XXXX$  and (b)  $ZZZZ$ .

Concerning the surface code specifically, elements of the phase factor 1 version of  $\hat{S}$  have the form  $XXXX$ ,  $XXX$  and  $XX$ , and  $ZZZZ$ ,  $ZZZ$  and  $ZZ$ . Measuring the phase factor 1 version of  $\hat{S}$  requires ancilla qubits [23], which we call syndrome qubits. See Fig. 1. We call the qubits in which logical information is stored data qubits. We separate  $\hat{S}$  into two generating sets: primal, the  $X$ -operators, and dual, the  $Z$ -operators. Primal and dual stabilizer generators are used to correct  $Z$ - and  $X$ -errors respectively. This is sufficient because an  $I$ -error is trivial and  $Y = \alpha XZ$ .

Consider Fig. 2. This is a surface code plate protecting one logical qubit. If a  $Z$ -error acts on the center data qubit then the primal stabilizer generators adjacent to it reverse phase causing two syndrome result changes. In larger surface code plates chains of errors can form, the stabilizer generators at the ends of which reverse phase. Chains can undetectably connect to boundaries. In Fig. 2 the shortest undetectable chain of errors has weight three. For example, an  $X$ -error on the center-left, center and center-right data qubit. We say ‘distance three’, write  $d = 3$ , and this is a measure of the strength of a surface code logical gate.

The normalizer of  $\hat{S}$  is the set of operators  $\mathcal{N}$  such that  $(\forall N \in \mathcal{N})[N, \hat{S}] = 0$ . This is the set of logical operators. By defining particular physical operators as particular logical operators we define basis logical states.

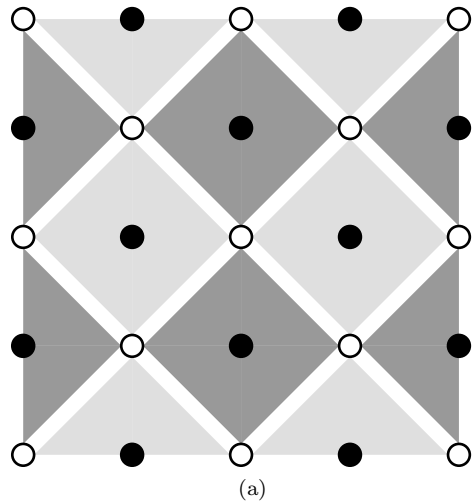


FIG. 2: A surface code plate protecting one logical qubit. Filled and empty circles denote syndrome and data qubits respectively. Darkly and lightly shaded shapes represent primal ( $X$ ) and dual ( $Z$ ) stabilizer generators respectively.

For example, in Fig. 2 a natural choice for  $X_L$  (logical  $X$ ) is any chain of  $X$ -operators from the left edge to the right that commutes with all dual ( $Z$ ) stabilizers.

The specific error correction of the surface code proceeds via pairing syndrome results to each other and to boundaries. This is because every correctible error may be decomposed into a set of error chains each of which causes either two syndrome result changes, or one due to the error chain connecting to a boundary. Note that an error chain that connects to two boundaries commutes  $\hat{S}$  and is hence uncorrectible. According that shorter error chains are more likely than longer ones, syndrome results should be paired using a minimum weight matching algorithm. Autotune, the tool we use for this task and which is briefly discussed in section III, uses Edmond’s minimum weight perfect matching algorithm [17, 24–26].

### III. NESTCHECK

A single round of measuring the stabilizers of Fig. 2 does not change the encoded data. In other words,  $I_L$  is applied. Less trivial logical gates involve rounds of error correction during which data qubits may be initialized, measured, swapped, and so on. Furthermore, we are not so fortunate that errors can only occur on data qubits between rounds of error correction: errors can occur on any qubit at any time, even measurements are prone to error.

In order to determine the error correction strength of a surface code logical gate we first construct a primal and a dual graph. The vertices of such a graph are the spacetime locations of potential syndrome result changes and the edges correspond to potential connections between syndrome result changes due to a single error. We

Command	Figure	Action
ACTIVE		Either SWAP-application due to a diagonally neighboring data qubit having a <i>SWAP_NW</i> , <i>SWAP_NE</i> , <i>SWAP_SW</i> or <i>SWAP_SE</i> command, or $\Lambda(X)$ -application due to measurement of neighboring stabilizer generators.
INACTIVE		Consider data qubit as nonexistent.
ADD_X		$ +\rangle$ -initialization followed by $\Lambda(X)$ -application due to measurement of neighboring stabilizer generators.
ADD_Z		$ 0\rangle$ -initialization followed by $\Lambda(X)$ -application due to measurement of neighboring stabilizer generators.
TRIM_X		$\Lambda(X)$ -application due to measurement of neighboring stabilizer generators followed by $X$ -basis-measurement.
TRIM_Z		$\Lambda(X)$ -application due to measurement of neighboring stabilizer generators followed by $Z$ -basis-measurement.
HAD		$\Lambda(X)$ -application due to measurement of neighboring stabilizer generators followed by $H$ -application.
SWAP_NW		SWAP-application of this data qubit and the syndrome qubit to the north followed by SWAP-application of the syndrome qubit to the north and the data qubit to the north-west.
SWAP_NE		SWAP-application of this data qubit and the syndrome qubit to the north followed by SWAP-application of the syndrome qubit to the north and the data qubit to the north-east.
SWAP_SW		SWAP-application of this data qubit and the syndrome qubit to the south followed by SWAP-application of the syndrome qubit to the south and the data qubit to the south-west.
SWAP_SE		SWAP-application of this data qubit and the syndrome qubit to the south followed by SWAP-application of the syndrome qubit to the south and the data qubit to the south-east.

(a)

Command	Figure	Action
ACTIVE		Either use syndrome qubit as an ancilla for stabilizer generator measurement where the data qubits included are those neighboring data qubits that have neither the command <i>INACTIVE</i> , nor <i>SWAP_NW</i> , <i>SWAP_NE</i> , <i>SWAP_SW</i> nor <i>SWAP_SE</i> , or SWAP-application due to a neighboring data qubit having one of the latter four commands.
INACTIVE		Consider syndrome qubit as nonexistent.

(b)

TABLE I: (a) Possible data qubit commands. (b) Possible syndrome qubit commands. Note that in figures stabilizers are represented as per Fig. 2 for convenience. This is not required in our set of commands because in any lattice of qubits we index the qubits with  $i$  and  $j$  such that if  $i + j \bmod 2 = 0$  we have a syndrome qubit and if also  $i \bmod 2 = 0$  we have a dual syndrome qubit.

construct this graph using the tool Autotune [27].

In the Autotune lexicon, our graph of vertices and edges is a nest of balls and sticks. From section II the data of error correction are the various measurements made during computation. Accordingly, Autotune creates a nest by processing many sets of measurements. A set is located in spacetime and has the property that if its measurements multiply to  $-1$ , as opposed to  $1$ , then its location is that of a syndrome result change. This implies either measurement error or phase-reversal of the associated stabilizer generator and is called a detection event. In a nutshell: qubits are simulated, during which course all possible errors are generated and propagated,

measurements of these qubits are placed in sets, all possible detection events are formed to create balls, and pairs of detection events generated by the same error are connected by a stick. We thus obtain our nest of balls and sticks. Note that the proximity of sets to temporal and spatial boundaries must be specified by the user so that unpaired detection events generate a stick to this boundary specifically.

The user must place every measurement in either two sets, or one set and a boundary set. Deciding when to create a set and in which set a particular measurement must be placed depends on the physical gate sequence the user is applying. This physical gate sequence can









Figure	Description
	$I_L$ -application.
	$ 0\rangle$ -initialization.
	$H$ -application.
	$Z$ -basis-measurement.
	$\Lambda(X)$ -application (left qubit is the control).
	SWAP-application.
	A set, whose measurements are those enclosed.
	The measurement enclosed is in a boundary set.

TABLE II: Notation scheme for parts of figures 3 to 7 that display physical gate sequences specified by frames.

be rather complex: a surface code computation typically involves introduction, deformation and elimination of boundaries, measurements in various bases, and single and double physical qubit gates. We desire a short list of commands to be given locally to physical qubits such that an arbitrary surface code computation can be specified. Table I details the list we use. Note that initializations specific to state-injection have not been included, but will be in future work.

We construct a surface code computation by writing a program. A program is a series of frames. A frame specifies a single round of error correction and is a list of physical qubits each with two data: a command and a boundary specification. We require boundary specifications for while Autotune can discern when a boundary set is required, it cannot discern which boundary set. Figs. 3 to 7 display small programs and elucidate how these specify gate sequences and sets. From these figures the logic of creating and placing measurements in sets can in part be inferred. We expand on this below.

There is some arbitrariness in how we use frames to specify sets. In sets containing two measurements, the measurements often have different times. The two measurements are specified by different frames and so the set is specified by these two frames conjointly. It is thus somewhat arbitrary which frame we choose to specify the boundary set that this set may connect to. We choose the frame executed at a later time.

It is convenient to introduce some terminology for discussing frames: If every data qubit has either the command `INACTIVE` or `ACTIVE` we call the frame an  $I_L$ -frame. Otherwise, we call the frame by the commands of the data qubits that are not `INACTIVE` or `ACTIVE`. For example, if some data qubit has the command `HAD` we call the frame a `HAD`-frame. Obviously, this is not the best terminology

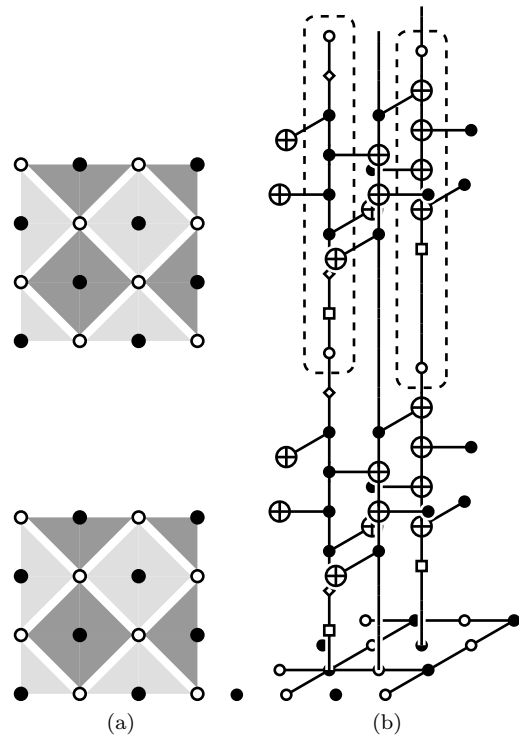


FIG. 3: A program consisting of two  $I_L$ -frames. (a) Representation of the program frames: Read upwards. See table I for the notation scheme. (b) Isometric view with upwards world lines: See table II for the notation scheme.

for frames in general: what do we call a frame in which some qubits have the command `ADD_X` while others have the command `ADD_Z`? Nevertheless, it serves us well in the discussion of boundary sets below.

In order to handle boundary sets, nonrepeating  $I_L$ -frames must often intersperse the frames of a program. By ‘nonrepeating  $I_L$ -frame’ we mean an  $I_L$ -frame in which more boundaries are specified than necessary were we to continually execute it. This is best illustrated by examining programs in which various frames are followed by  $I_L$ -frames. There are four cases:

(i) An  $I_L$ -frame followed by  $I_L$ -frames: Obviously, of the  $I_L$ -frames following the  $I_L$ -frame none needs to be nonrepeating. See Fig. 3.

(ii) An `ADD_X`- or `ADD_Z`-frame followed by  $I_L$ -frames: Consider specifically the `ADD_X`-frame shown in Fig. 4(d). Syndrome qubits are activated in this frame. Since we are  $|+\rangle$ -initialising data qubits, the first syndrome result of a dual syndrome qubit activated in this frame is random and must be placed in a boundary set and a set that connects to this boundary. The user must specify which boundary set in the `ADD_X`-frame, and while Autotune can discern that the connection mentioned is required it cannot discern which boundary set must be connected to. The user must therefore specify the connection in the directly following  $I_L$ -frame. Such boundary information is

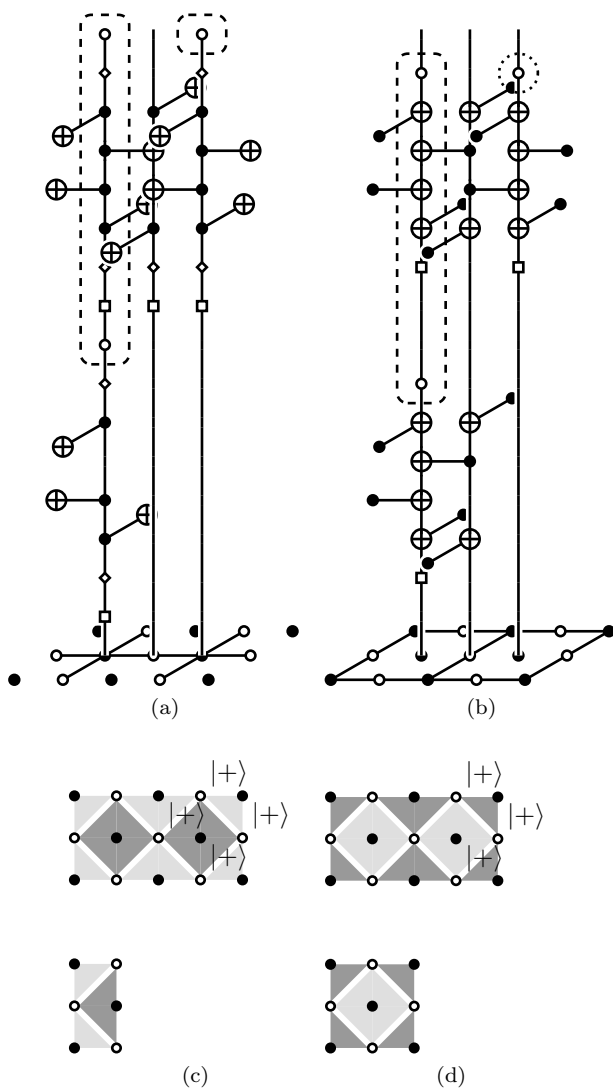


FIG. 4: Each pair (a)-(c) and (b)-(d) is a program consisting of an  $I_L$ -frame followed by a  $ADD_X$ -frame. (a) and (b) are isometric views with upwards world lines: See table II for the notation scheme. (c) and (d) are representations of the program frames: Read upwards. See table I for the notation scheme.

not required in a repeating  $I_L$ -frame. Thus the  $I_L$ -frame that directly follows the  $ADD_X$ - or  $ADD_Z$ -frame needs to be nonrepeating, all other following  $I_L$ -frames can be repeating.

(iii) A  $TRIM_X$ - or  $TRIM_Z$ -frame followed by  $I_L$ -frames: Consider specifically the  $TRIM_X$ -frame in Fig. 5(d). In the directly following frame, syndrome qubits are deactivated. We cannot use the  $X$ -basis-measurements of data qubits to construct dual ( $Z$ ) syndrome results. The final syndrome result of a dual syndrome qubit deactivated in the directly following  $I_L$ -frame must hence be placed in a boundary set and a set that connects to this boundary. Both of these sets are specified by the  $TRIM_X$ -frame. Thus none

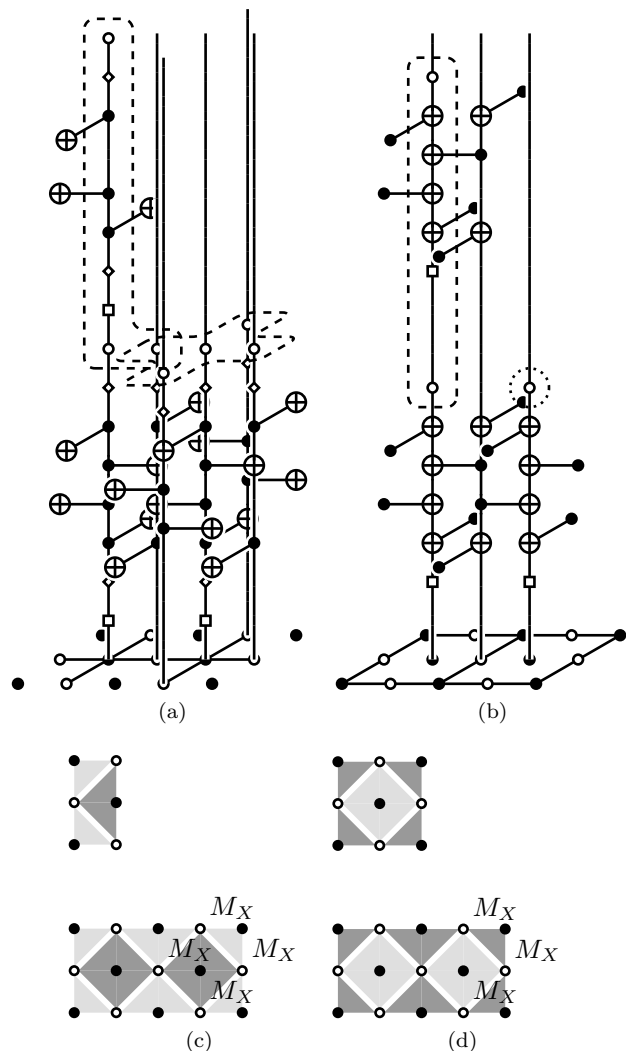


FIG. 5: Each pair (a)-(c) and (b)-(d) is a program consisting of an  $TRIM_X$ -frame followed by a  $I_L$ -frame. (a) and (b) are isometric views with upwards world lines: See table II for the notation scheme. (c) and (d) are representations of the program frames: Read upwards. See table I for the notation scheme.

of the  $I_L$ -frames that follows the  $TRIM_X$ - or  $TRIM_Z$ -frame needs to be nonrepeating.

(iv) A  $HAD$ -frame followed by a  $SWAP_{NW}$ -,  $SWAP_{NE}$ -,  $SWAP_{SW}$ - or  $SWAP_{SE}$ -frame followed by  $I_L$ -frames: Consider specifically the  $SWAP_{NW}$ -frame in Fig. 6(b). In the directly following frame, syndrome qubits are activated. Ideally, the first syndrome result of each syndrome qubit activated in the directly following frame should be matched with that of the previous  $HAD$ -frame diagonally offset from it. This would involve, however, converting a primal nest into a dual nest and vice versa, which would in practice be quite a bit of effort code. Perhaps in future research we shall concern ourselves with this, but for the moment we use a shortcut. We simply consider activated syndromes as entirely new. The first syndrome result of

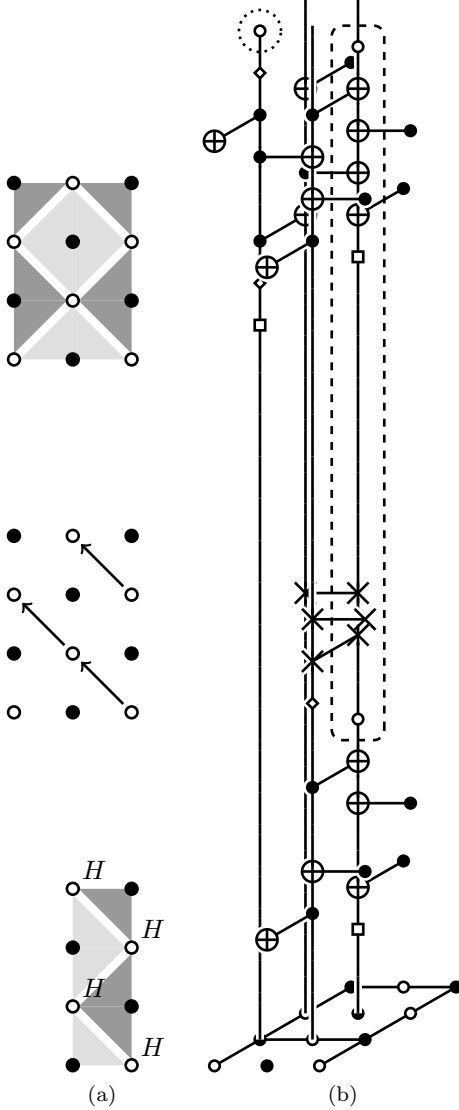


FIG. 6: A program consisting of a HAD-frame followed by a SWAP\_NW-frame followed by an  $I_L$ -frame. Note that these frames are to be understood as possibly extending an arbitrary distance in the north, west, east and south directions, lest data qubits appear from and disappear to nowhere (see Fig. 11(d) of appendix B for an example of a complete swapping). (a) Representation of the program frames: Read upwards. See table I for the notation scheme. (b) Isometric view with upwards world lines: See table II for the notation scheme.

each syndrome qubit activated in the directly following frame is then considered random and must be placed in a boundary set and a set that connects to this boundary. This situation is similar to case (i) but one frame onwards. Thus two of the  $I_L$ -frames that directly follow the SWAP\_NW-, SWAP\_NE-, SWAP\_SW- or SWAP\_SE-frame need to be nonrepeating.

A further note is necessary on case (iv): The HAD-frame requires more boundaries than one might naïvely expect to

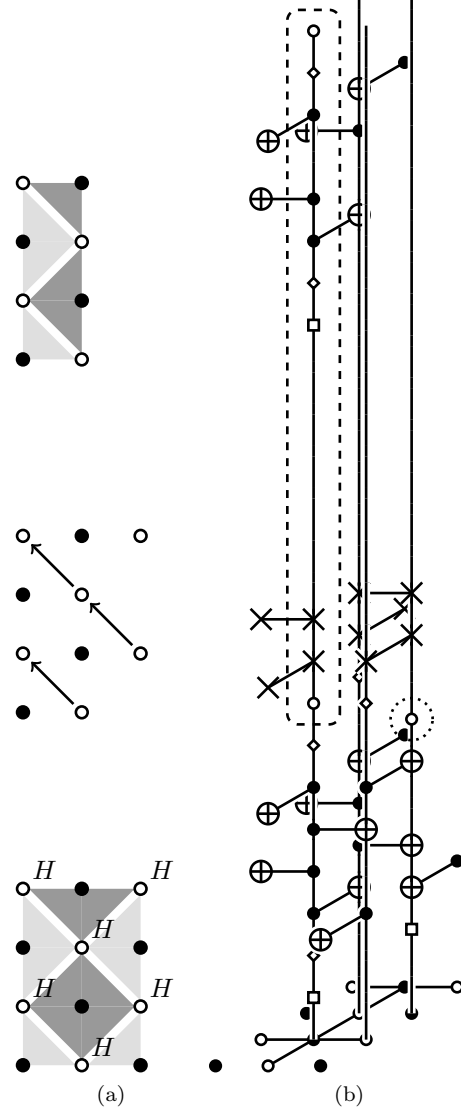


FIG. 7: A program consisting of a HAD-frame followed by a SWAP\_NW-frame followed by an  $I_L$ -frame. Note that these frames are to be understood as possibly extending an arbitrary distance in the north, west, east and south directions, lest data qubits appear from and disappear to nowhere (see Fig. 11(d) of appendix B for an example of a complete swapping). (a) Representation of the program frames: Read upwards. See table I for the notation scheme. (b) Isometric view with upwards world lines: See table II for the notation scheme.

be specified. Consider specifically the SWAP\_NW-frame in Fig. 7(b). In this frame syndrome qubits are deactivated. Since we are using a shortcut, the final syndrome result of each syndrome qubit deactivated in this frame must be placed in a boundary set and a set that connects to this set. Both of these sets are specified by the previous frame, the HAD-frame. Thus the HAD-frame must include boundary information to this effect.

An indispensable tool used in debugging the logic for

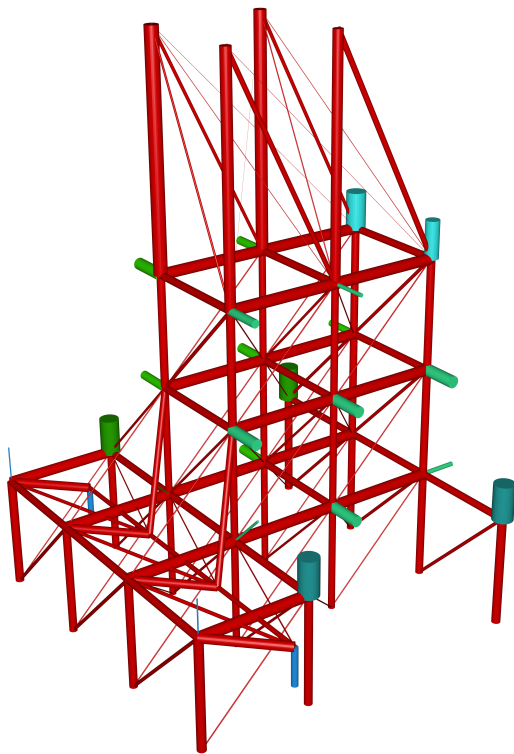


FIG. 8: Color online. Blender model of a section of the primal nest for  $d = 3 H_L$  as presented in appendix B. Thicker cylinders (sticks) represent more probable connections between potential syndrome result changes (balls) due to a single error. Red cylinders represent sticks between sets, differently colored cylinders represent sticks between a set and a boundary set. In this nest section we see trimming and the beginning of swapping. There are more sets than usual in a trimming time-slice, hence the offset cylinder intersection points.

handling sets is a simple Blender visualizer we have developed [27]. This tool creates a 3D blender model of a nest so that we can see whether the correct boundaries have been specified and the correct connections exist. Fig. 8 is such a model of a section of the primal nest for  $d = 3 H_L$  as set out in appendix B.

With the primal and dual nests built for a particular surface code logical gate we then need to find the shortest chain between any two boundaries and the smallest topologically nontrivial ring. The length of the smaller of these two is the distance of this surface code logical gate and so the error correction strength.

Finding the shortest chain between two boundaries is simple. We loop over pairs of boundaries and perform a breadth first search between them.

As to finding the smallest topologically nontrivial ring the situation is not quite so undemanding and we have not yet implemented such a search. This is not to invalidate Nestcheck, however, for rings are generally easy to see. Nevertheless, without this ability Nestcheck cannot be considered complete.

In future work we plan to search for a set of smallest topologically distinct and nontrivial rings. An outline of our prospective method is thus: The ‘hole’ around which a topologically nontrivial ring in a nest of one type can exist is itself a ring, or at least a closed structure [28], of the other type. This latter ring can be specified by the user. The task is then reduced to, for each input ring of a certain type, looping over an appropriately constructed set of rings in the nest of the other type and checking whether each interlocks with the input ring. The conceptually principal part of this algorithm is a method for determining whether a given primal ring interlocks with a given dual ring.

Nestcheck has been tested extensively on a wide variety of physical gate sequences. Furthermore, as an example, we have run Nestcheck on a proposal for  $d = 3 H_L$  (see appendix B). Nestcheck found that this proposal is  $d = 3$  as purported.

#### IV. CONCLUSION

We have reported a new tool Nestcheck capable of analysing an arbitrary surface code computation and determining the minimum number of errors required to cause failure. 3D topological cluster states may also be analysed since the data that Nestcheck analyses is created using Autotune. In future research, surface code computations consisting of many qubits shall be constructed, for which it is highly nontrivial to check the strength of error correction. Nestcheck shall therefore be of utility in this endeavour. Furthermore, using the framework of Nestcheck (programs, frames, and so on), we are able to easily specify a complex surface code computation thus enabling simulation of such to be relatively quickly and painlessly written.

#### Acknowledgments

This research was conducted by the Australian Research Council Centre of Excellence for Quantum Computation and Communication Technology (project number CE110001027), with support from the United States National Security Agency and the United States Army Research Office under contract number W911NF-08-1-0527. Supported by the Intelligence Advanced Research Projects Activity (IARPA) via Department of Interior National Business Center contract number D11PC20166. The United States Government is authorized to reproduce and distribute reprints for governmental purposes notwithstanding any copyright annotation thereon. Disclaimer: The views and conclusions contained herein are those of the authors and should not be interpreted as necessarily representing the official policies or endorsements, either expressed or implied, of IARPA, DoI/NBC, or the United States Government.

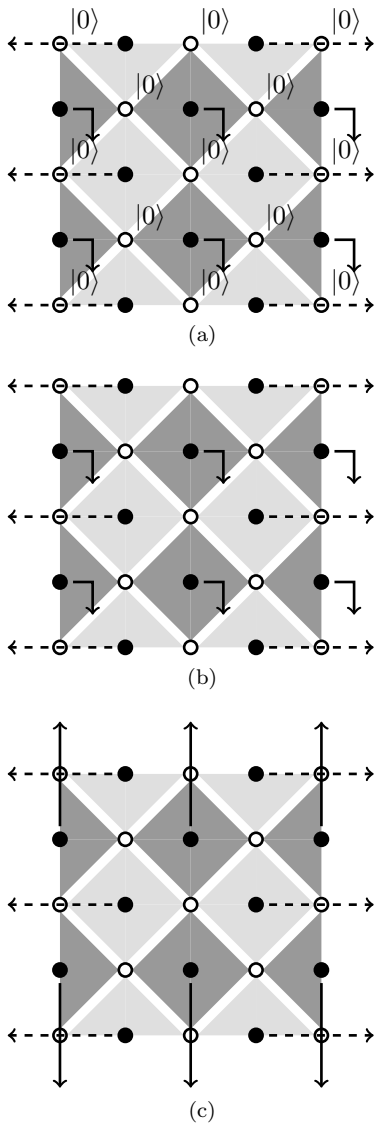


FIG. 9: Full program for simulating the surface code plate of Fig. 2. Read (a), (b) then (c). See table I for the notation scheme. Arrows represent boundary specifications: solid and dashed for primal and dual respectively, and bent and straight for temporal and spatial respectively. We see three primal boundaries: a temporal one, one along the top and one along the bottom. We see two dual boundaries: one along the left and another along the right. Note that in general spatiotemporal boundary specifications are possible.

#### Appendix A: Full program for a distance three plate

Fig. 9 details an entire program for simulating the surface code plate of Fig. 2. Boundary specifications have

been included. The final frame, Fig. 9(c), is repeating in the sense of section III.

#### Appendix B: Distance three logical hadamard

A scheme for  $d = 7 H_L$  is presented in [29]. We adapt this to  $d = 3$ . Besides nonrepeating  $I_L$ -frames (see section III, Figs. 10 to 12 present this adaptation.

#### Appendix C: Checking the logic of specific surface code logical gates

There would be little point in checking the error correction strength of a proposal for surface code logical gate without checking whether it is indeed the logical gate purported. Future research shall potentially yield a general tool for this task [28], but for the moment we resort to specific methods.

Excepting initializations specific to state-injection, the physical gates of an arbitrary surface code computation are in the clifford group. Algorithms for efficiently simulating clifford group quantum circuits have been developed and implemented, and are available for download. We currently use Graphsim [30]. Constructing a Graphsim simulation is simple: we declare a qubit register and then call our gate sequence.

To view the state of the qubit register at a point during simulation there are two methods. We may either print a table of stabilizers, or simply create a duplicate of the qubit register and measure all the qubits in an appropriate basis. Since we are checking rather than investigating logic we choose the latter method.

Take  $H_L$  as an example. Here we must check whether the gate maps  $|0\rangle$ ,  $|1\rangle$ ,  $|+\rangle$  and  $|-\rangle$  to  $|+\rangle$ ,  $|-\rangle$ ,  $|0\rangle$  and  $|1\rangle$  respectively. Consider the case  $|0\rangle \mapsto |+\rangle$ : We initialize the logical qubit to  $|0\rangle$  and then apply the gate sequence of  $H_L$ , during which course byproduct-operators [13] accrue. Then we measure in the  $X$ -basis each qubit to which  $X_L$  is nontrivial and check whether the multiple of these measurements with those associated with the appropriate byproduct-operators is 1. Success is declared if so, otherwise failure.

This method of checking logic is stochastic. In order to reliably check using this method, then, we must apply it a large number of times. If failure is declared even once then the proposal fails entirely.

[1] R. P. Feynman, *Int. J. Theor. Phys.* **21**, 467 (1982).  
 [2] D. Deutsch, *Proc. R. Soc. Lond. A* **400**, 97 (1985).

[3] P. W. Shor, in *Proc. 35th Annual Symposium on Foundations of Computer Science* (IEEE Computer Society Press,



- Los Alamitos, CA, 1994), pp. 124–134, quant-ph/9508027.
- [4] A. Berthiaume, D. Deutsch, and R. Jozsa, in *Physics and Computation, 1994. PhysComp'94, Proceedings, Workshop on* (IEEE, 1994), pp. 60–62.
- [5] P. W. Shor, Phys. Rev. A **52**, R2493 (1995).
- [6] A. M. Steane, Phys. Rev. Lett. **77**, 793 (1996).
- [7] E. Knill, R. Laflamme, and W. Zurek, quant-ph/9610011 (1996).
- [8] D. Aharonov and M. Ben-Or, Proc. ACM STOC **29**, 176 (1997), quant-ph/9611025.
- [9] S. B. Bravyi and A. Y. Kitaev, quant-ph/9811052 (1998).
- [10] E. Dennis, A. Y. Kitaev, A. Landahl, and J. Preskill, J. Math. Phys. **43**, 4452 (2002), quant-ph/0110143.
- [11] R. Raussendorf, J. Harrington, and K. Goyal, Ann. Phys. **321**, 2242 (2006), quant-ph/0510135.
- [12] R. Raussendorf, J. Harrington, and K. Goyal, New J. Phys. **9**, 199 (2007), quant-ph/0703143.
- [13] A. G. Fowler and K. Goyal, Quant. Info. Comput. **9**, 721 (2009), arXiv:0805.3202.
- [14] A. G. Fowler, M. Mariantoni, J. M. Martinis, and A. N. Cleland, Phys. Rev. A **86**, 032324 (2012), arXiv:1208.0928.
- [15] B. Schumacher, Physical Review A **51**, 2738 (1995).
- [16] D. S. Wang, A. G. Fowler, and L. C. L. Hollenberg, Phys. Rev. A **83**, 020302(R) (2011), arXiv:1009.3686.
- [17] A. G. Fowler, A. C. Whiteside, and L. C. L. Hollenberg, arXiv:1202.5602 (2012).
- [18] D. Gottesman, Ph.D. thesis, Caltech (1997), quant-ph/9705052.
- [19] D. Gottesman, Phys. Rev. A **57**, 127 (1998), quant-ph/9702029.
- [20] R. Raussendorf and J. Harrington, Phys. Rev. Lett. **98**, 190504 (2007), quant-ph/0610082.
- [21] P. Kaye, R. Laflamme, and M. Mosca, *An Introduction to Quantum Computing* (Oxford University Press, Great Clarendon Street, Oxford OX2 6DP, 2007), ISBN 9780198570493.
- [22] M. A. Nielsen and I. L. Chuang, *Quantum Computation and Quantum Information* (Cambridge University Press, Cambridge, 2000).
- [23] D. P. DiVincenzo and P. W. Shor, Phys. Rev. Lett. **77**, 3260 (1997), quant-ph/9605031.
- [24] J. Edmonds, Canad. J. Math. **17**, 449 (1965).
- [25] J. Edmonds, J. Res. Nat. Bur. Standards **69B**, 125 (1965).
- [26] A. G. Fowler, A. C. Whiteside, and L. C. L. Hollenberg, Phys. Rev. Lett. **108**, 180501 (2012), arXiv:1110.5133.
- [27] A. G. Fowler, A. C. Whiteside, A. L. McInnes, and A. Rabhani, arXiv:1202.6111 (2012).
- [28] A. G. Fowler and S. J. Devitt, arXiv:1209.0510 (2012).
- [29] A. G. Fowler, arXiv:1202.2639 (2012).
- [30] S. Anders and H.-J. Briegel, Phys. Rev. A **73**, 022334 (2006), quant-ph/0504117.

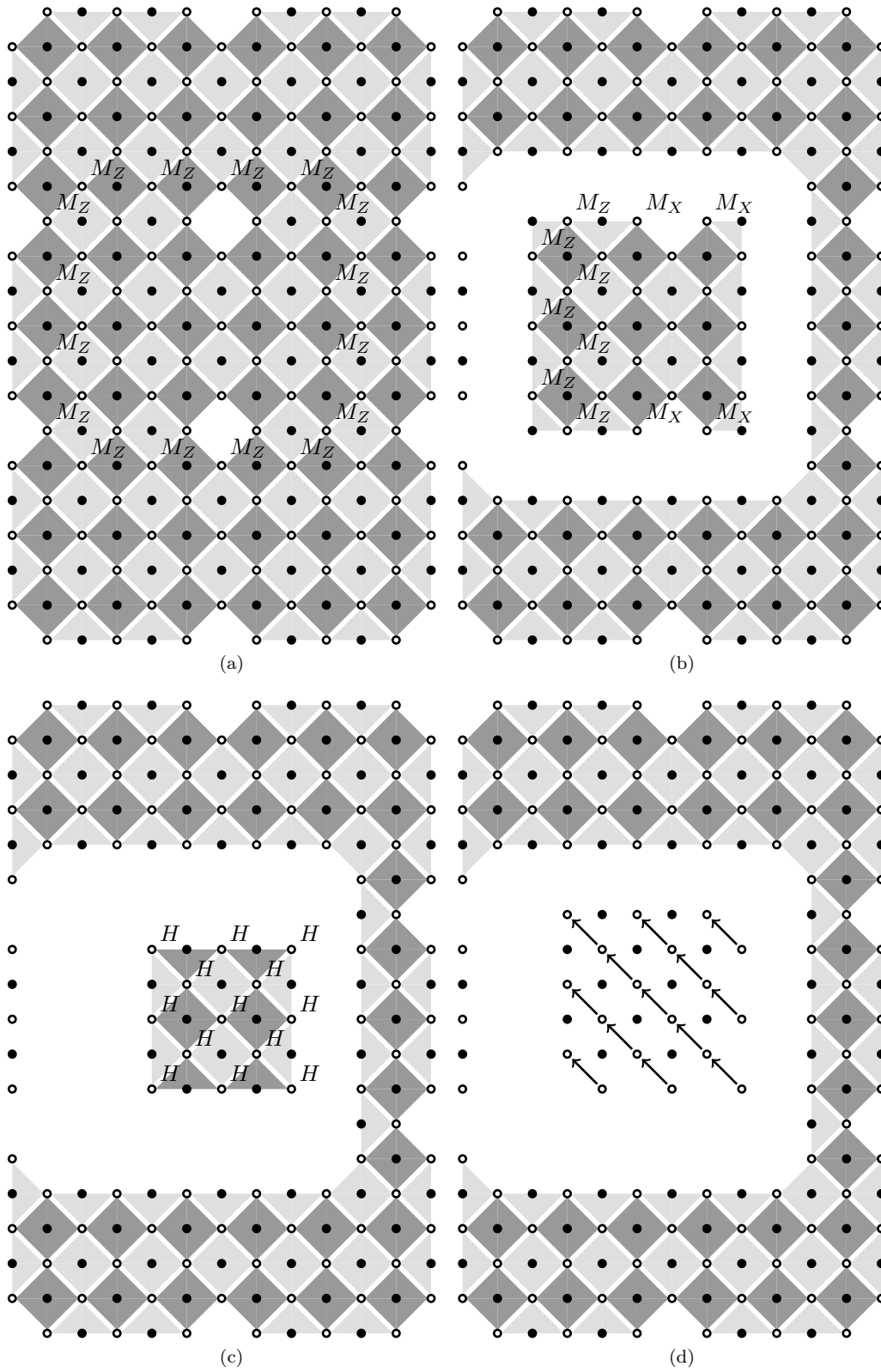


FIG. 10: Frames for simulating  $d = 3 H_L$ . See table I for the notation scheme.

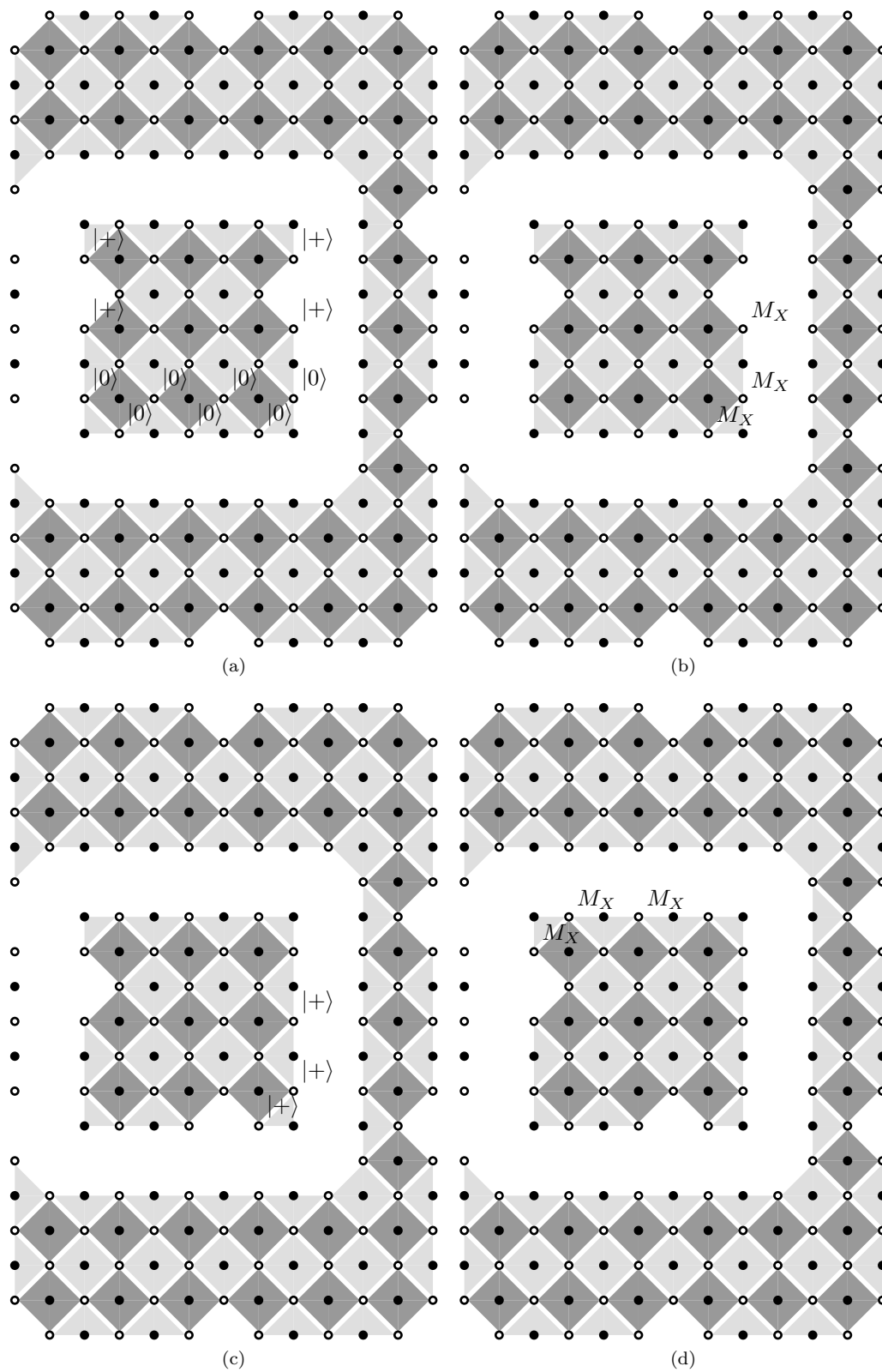


FIG. 11: Frames for simulating  $d = 3 H_L$ . See table I for the notation scheme.

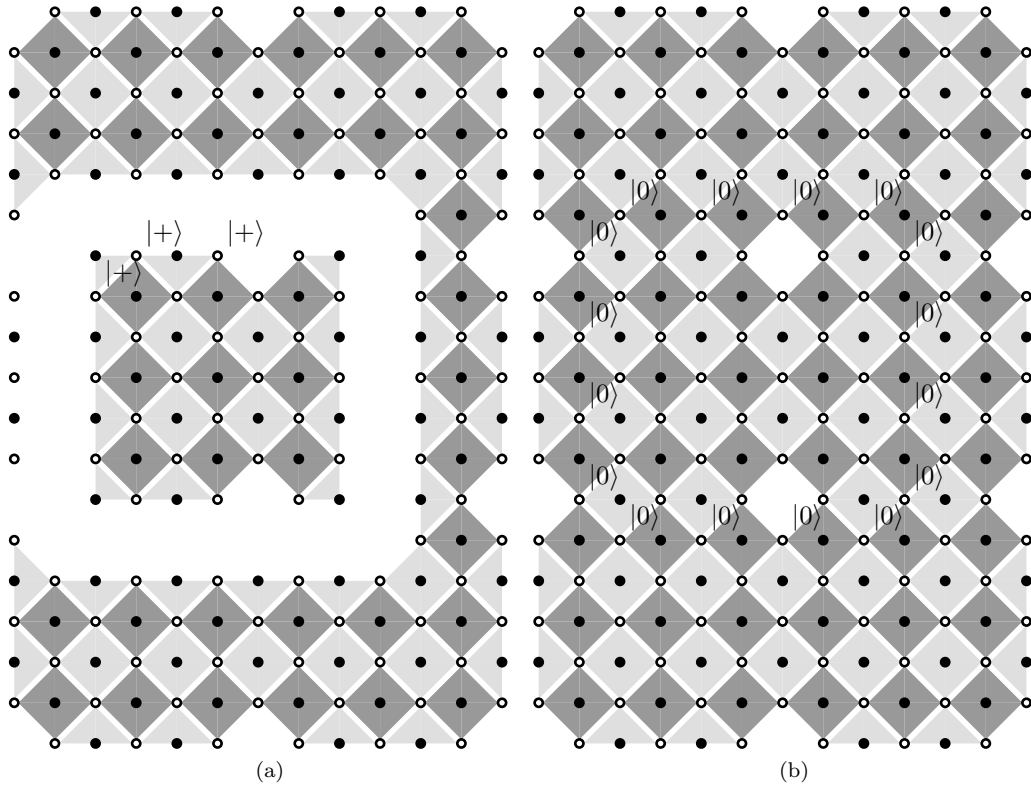


FIG. 12: Frames for simulating  $d = 3$   $H_L$ . See table I for the notation scheme.